6th International Conference on Earthquake Geotechnical Engineering
1-4 November 2015
Christchurch, New Zealand

Numerical Simulations of Liquefaction Effects on Piled Bridge Abutments

R. J. Armstrong[1], R.W. Boulanger[2]

ABSTRACT

Earthquake-induced deformations of piled bridge abutments in approach embankments underlain by liquefied soils may be reduced relative to free-field deformation values by the restraining forces from the piles and bridge superstructure. Three dynamic centrifuge model tests demonstrating pile pinning effects in approach embankments were numerically simulated using two-dimensional finite difference models. Each centrifuge model was composed of two identical embankments underlain by liquefiable soil, one with a pile group and the other without. Agreement between the numerical simulations and centrifuge model results were assessed through comparison of accelerations, pore water pressures, displacements, and pile bending moments for both the piled and non-piled embankments. The capabilities and limitations in the numerical modeling procedures for the seismic evaluation of piled and non-piled bridge approach abutments are discussed.

Introduction

The seismic design of piled bridge abutments in approach embankments underlain by liquefiable soils requires estimates of the potential deformations imposed on the system. Restraining forces from the piles and bridge superstructure can reduce the deformations of piled bridge abutments relative to free-field deformation values. These pile pinning effects have been observed in the field (e.g., Cubrinovski et al. 2014) and centrifuge model tests (Armstrong et al. 2013), and are incorporated in some simplified design procedures.

This paper describes the results of nonlinear deformation analyses (NDA) of three dynamic centrifuge model tests of piled and non-piled approach embankments affected by earthquake-induced liquefaction. The three dynamic centrifuge tests, described previously in Armstrong et al. (2013), each consisted of two identical embankments underlain by liquefiable soil, one with a pile group and the other without. The centrifuge results were used by Armstrong et al. (2013, 2014) to evaluate both an NDA model using the numerical platform FLAC (Itasca 2011) with the user-defined constitutive model UBCSAND (Byrne et al. 2004, Beaty and Byrne 2011) and an equivalent static analysis (ESA) design procedure. This paper presents results of NDAs using the same numerical model, except now with the user-defined constitutive model PM4Sand (Boulanger and Ziotopoulou 2015). The centrifuge testing program and NDA modeling procedures are described, followed by comparisons of the measured and simulated responses. These comparisons provide a basis for evaluating the capabilities and limitations in the numerical modeling procedures for the seismic performance of piled and non-piled bridge approach embankments.

[1]Assistant Professor, California State University, Sacramento, USA, richard.armstrong@csus.edu
[2]Professor, University of California, Davis, USA, rwboulanger@ucdavis.edu

Centrifuge Tests

The centrifuge testing program is summarized in Armstrong et al. (2013) with the experimental data available in Chang et al. (2007) and Gulerce et al. (2007a, 2007b). All tests were performed at a centrifugal acceleration of 60g. Standard scaling laws are followed and results are presented in prototype units unless otherwise specified. Each centrifuge model was comprised of two identical approach embankments of dry sand separated by a channel, as shown by the photographs in Fig. 1 and the model section in Fig. 2. One embankment had a pile group that extended through the underlying saturated loose sand layer and into saturated dense sand. All three centrifuge tests had essentially the same soil properties and soil geometry but different pile-group configurations or input motions: (1) test Kobe_1X6 had a single row of six 0.72-m diameter piles in the piled embankment and was shaken with a scaled version of a ground motion recording from the 1995 Kobe earthquake, (2) test Kobe_2X4 had two rows of four 1.22-m diameter piles with a connecting pile cap in the piled embankment and was shaken by the same motion as the first test, and (3) test Sine_2X4 had the same pile group as the second test but was shaken by an input motion comprised of packets of sine waves of varying amplitudes. All embankments were 8 m above the channel at the crest and 11 m above the channel at the model container wall, with a crest width of 12 m and side slopes of 2 to 1 (horizontal to vertical) in all directions. The embankments were comprised of dry, coarse, dense Monterey sand. The embankments were underlain, in sequence, by a 1.3-m-thick compacted, non-plastic silt layer, a 5-m-thick loose sand layer, a 0.7-m-thick compacted silt layer, and 17-m-thick dense sand layer. A channel 12 m wide was left between the two embankments in the middle of the container to reduce interactions between the two embankments. The pore fluid was a methylcellulose solution with a viscosity about 20 times that of water. The water table was at the base of the embankments.

Numerical Model Development

The two-dimensional (2D) NDAs were performed using the program FLAC (Itasca 2011) with the user-defined constitutive model PM4Sand. The numerical models are essentially identical to those used by Armstrong et al. (2013) with the exception of the constitutive model for the sands; i.e., the finite difference mesh (Fig. 2), soil permeabilities, and properties for the centrifuge container, piles, and soil-pile interface elements are the same. Piles were modeled using linear elastic beam elements, with a 2D equivalent arrangement based on multiplying the stiffness and mass of the piles by the number of out-of-plane piles divided by the equivalent crest width. Piles are connected to the soil mesh by normal and shear coupling springs which allow the soil to move relative to the piles. Initial static stress conditions were established by modeling the sequence of model construction and progressive increase in g-field on the centrifuge. Dynamic analyses were performed with 0.5% Rayleigh damping at the predominate frequency of the model of 1.5 Hz. Additional details on the simulation steps and analysis parameters are in Armstrong et al. (2013).

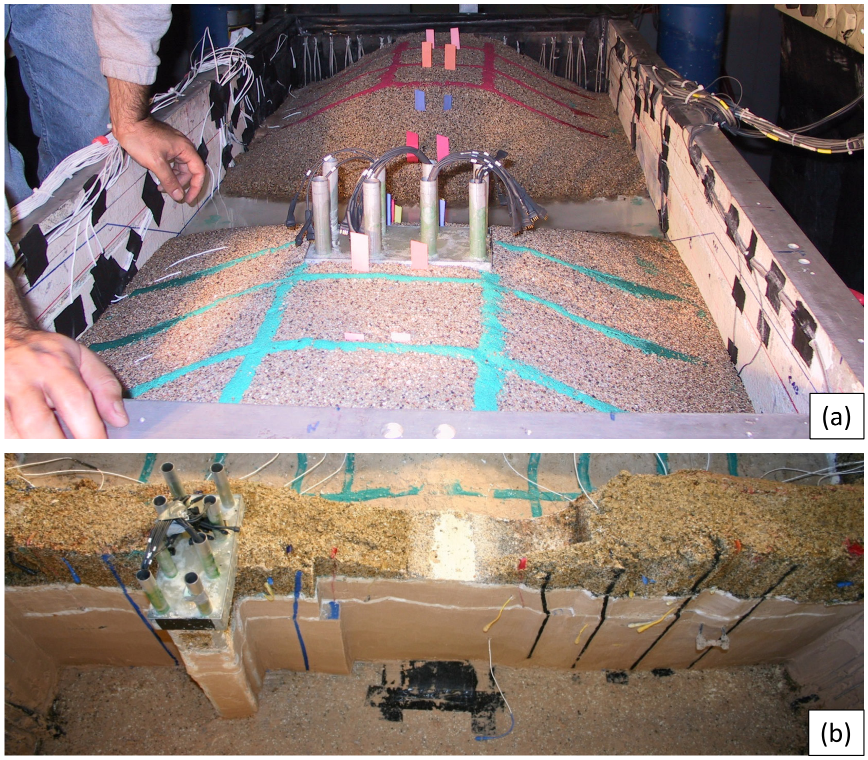

Figure 1. Model Kobe_2x4: (a) before testing, and (b) excavation after testing

The constitutive model PM4Sand used for simulating all soils in the model is a stress-ratio controlled, critical state compatible, bounding surface plasticity model developed primarily for earthquake engineering applications. The development and calibration procedures for Version 2 of the model are described in Boulanger and Ziotopoulou (2013) and Ziotopoulou and Boulanger (2013), whereas recent revisions for Version 3 are described in Boulanger and Ziotopoulou (2015). The analyses presented herein were performed with Version 3.

Calibration of PM4Sand for the loose and dense Nevada sands was based on cyclic and monotonic laboratory tests and shear wave velocity data summarized in Armstrong et al. (2013) and Kamai and Boulanger (2013). The calibrated parameters are listed in Table 1; all other parameters retained the default values specified in the model. These calibrations correspond to a normalized V_{s1} of 179 m/s (loose) and 192 m/s (dense) and cyclic resistance ratios of 0.09 (loose) and 0.24 (dense) against triggering of 3% peak shear strain in 15 uniform cycles of undrained simple shear loading.

Properties for the dense dry sand in the embankments are listed in Table 1, and properties of the two nonplastic silt layers were taken as equal to those for the loose Nevada sand.

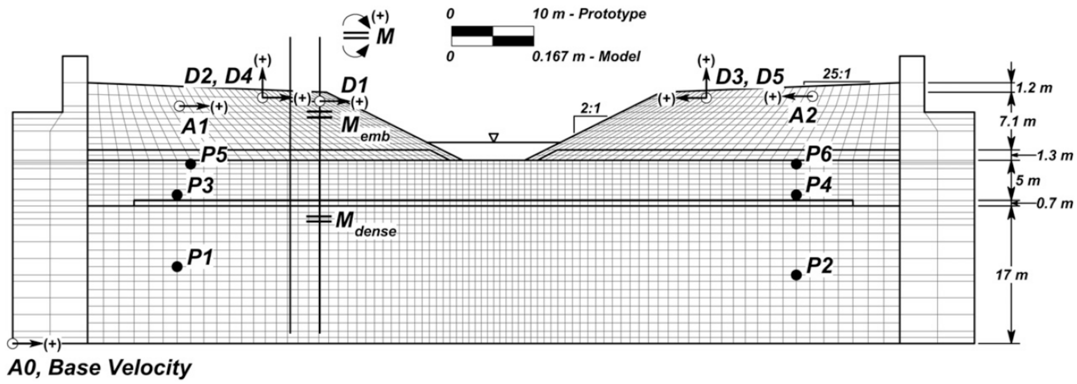

Figure 2. Finite difference mesh for models Kobe_2x4 and Sine_2x4 showing locations and sign conventions for instrument time series

Table 1. Parameters specified for PM4Sand; all other parameters retain default values listed in the manual by Boulanger and Ziotopoulou (2015)

	Loose Nevada Sand	**Dense Nevada Sand**	**Dense Monterey Sand**
e_{max}	0.793	0.793	0.82
e_{min}	0.485	0.485	0.54
D_R	40%	80%	100%
ϕ'_{cv}	32°	32°	33°
Q	9.5	9.5	9.5
R	0.7	0.7	0.7
G_o	735	878	771
h_{po}	0.056	0.009	0.009

Analysis Results

Measured and computed time series for accelerations, pore pressures, displacements, and pile bending moments for all three centrifuge models are shown in Figure 3. The locations and sign conventions for all instruments are shown on the mesh in Figure 2.

Computed acceleration responses are in reasonable agreement with measured values throughout the models. Response spectra for the measured and computed accelerations at several points in all three centrifuge models are shown in Figure 4. The spectra for the measured and computed motions show that the longer-period components of motions were stronger at the embankments than at the model base, which is consistent with the expected effects of liquefaction.

The computed excess pore water pressures were generally higher than those measured in the dense sand layer, comparable to those measured near the bottom of the loose sand layer during strong shaking, and higher than those measured near the top of the loose sand layer. The discrepancy between the computed and measured pore pressures could be partly due to inadequate saturation of transducers close to the water table surface (i.e., P5 and P6) and three-

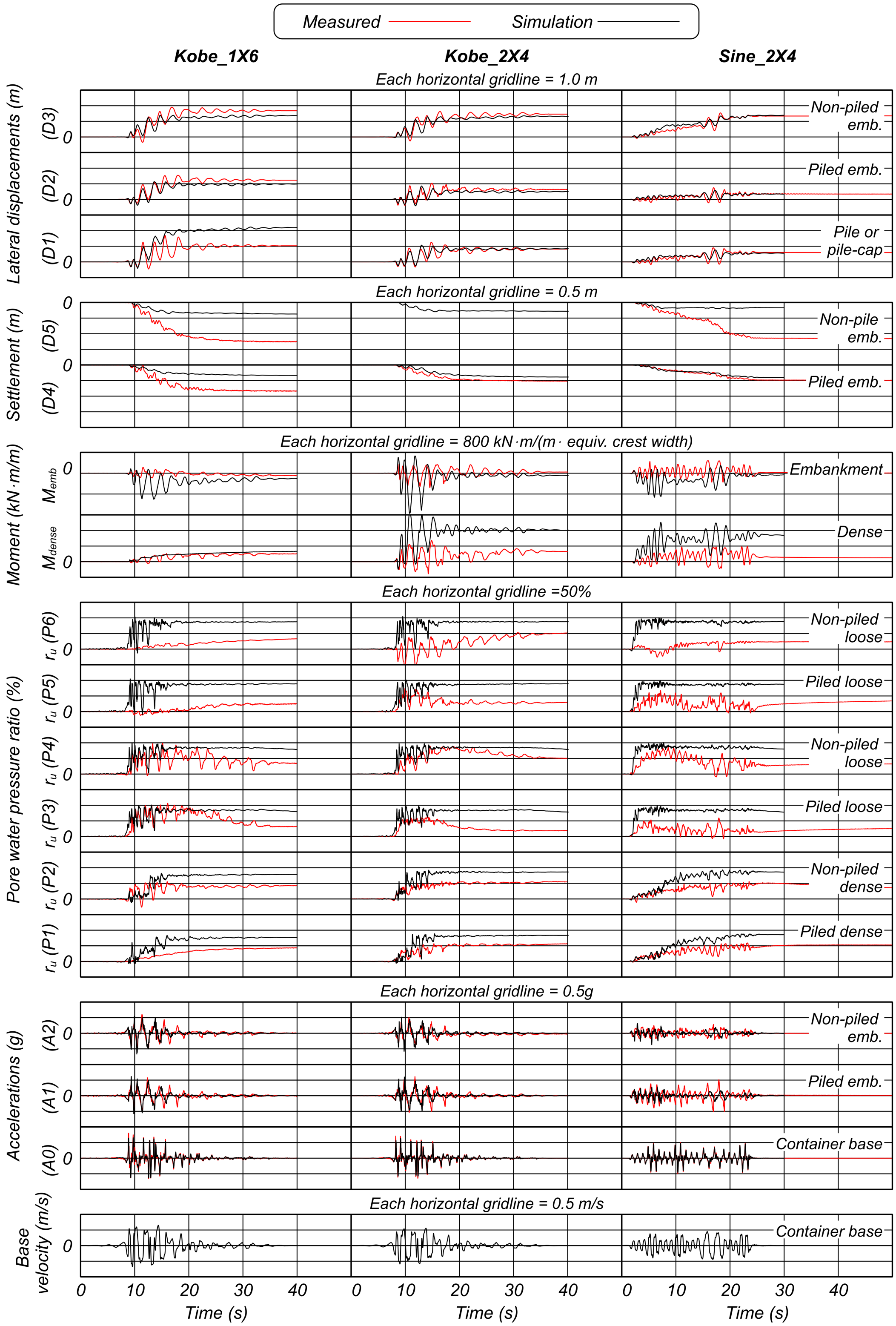

Figure 3. Measured and computed responses (locations and sign convention in Figure 2)

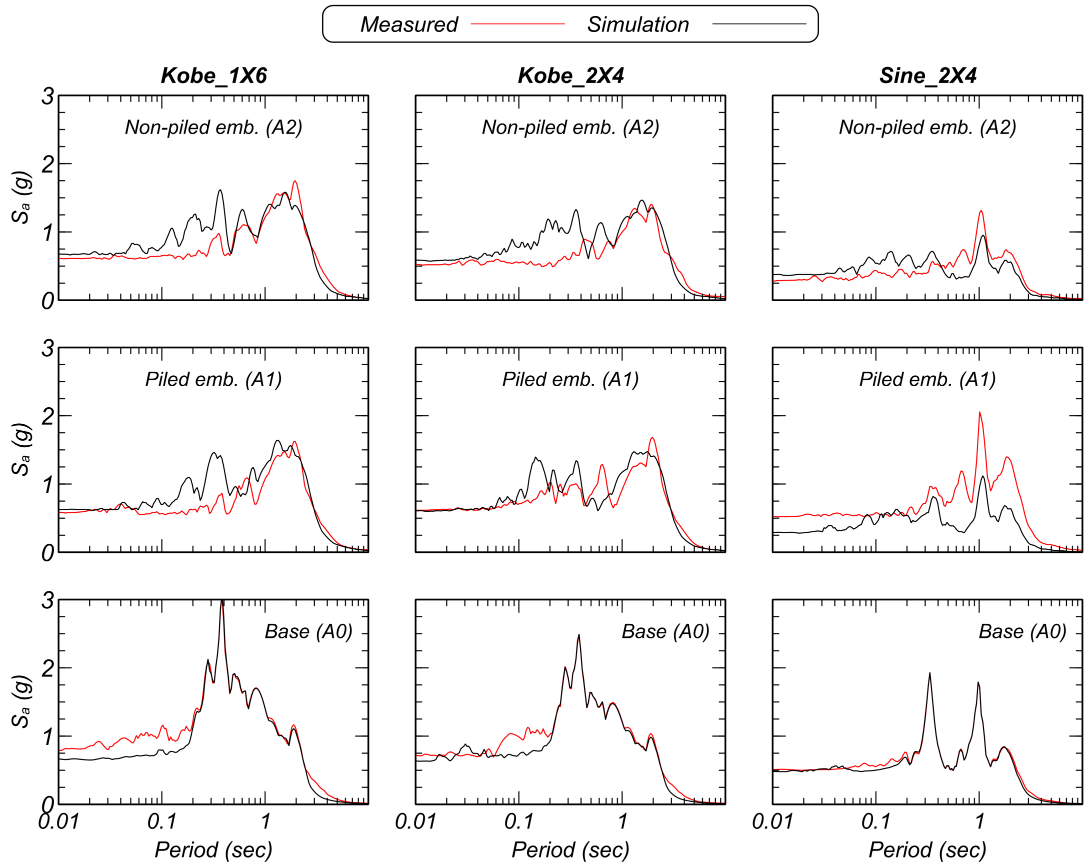

Figure 4. Spectral accelerations (5% damped) of measured and computed accelerations at the base, in the piled embankment, and in the non-piled embankment for each centrifuge test

dimensional (3D) effects not being included in the simulations; i.e., out-of-plane shear stresses in the centrifuge test would tend to limit the maximum residual pore water pressures and out-of-plane pore water flow would enable pore pressures to dissipate more quickly.

The computed and measured lateral displacements at the pile-head (Kobe_1X6) or pile-cap (Kobe_2X4 and Sine_2X4) were generally in good agreement, whereas the computed settlements at the embankment crests tended to be smaller than the measured values. Embankment side slopes developed significant out-of-plane deformations in the centrifuge tests, which is a mechanism that the 2D NDAs do not account for.

Deformed meshes with contours of maximum shear strain at the end of shaking for models Kobe_1X6, Kobe_2X4, and Sine_2X4 are shown in Figure 5. The NDAs captured the overall deformation patterns observed in the centrifuge tests, including the slumping and spreading of the embankments toward the central channel, the local slumping of the embankments on the channel side of any of the pile foundations, and the heaving along the central channel.

Profiles of measured and computed pile bending moments at the time of peak bending moment are shown in Figure 6. The computed peak moments were generally greater than those measured.

The NDA predicted a strong reversal of bending moments in the embankment (upper portion of the pile); however, the measured bending moments showed relatively small bending moments over this interval. The over-prediction of the reversed bending moments within the embankment is attributed to the differences in the predicted soil displacement profiles throughout the model.

Conclusions

Presented were results of 2D nonlinear deformation analyses (NDAs) of three dynamic centrifuge model tests of piled and non-piled bridge approach embankments affected by earthquake-induced liquefaction. The NDAs were performed using the numerical platform FLAC (Itasca 2011) with the user-defined constitutive model PM4Sand – Version 3 (Boulanger and Ziotopoulou 2015). The 2D NDAs reproduced the primary behaviors of these centrifuge tests, such as the patterns of deformation and the relative differences between deformations in the piled and non-piled embankments (i.e., pile pinning). Differences between the computed and measured responses were consistent with the expected limitations of a 2D approximation of the 3D centrifuge models, wherein out-of-plane deformations or pore water seepage would not be properly accounted for.

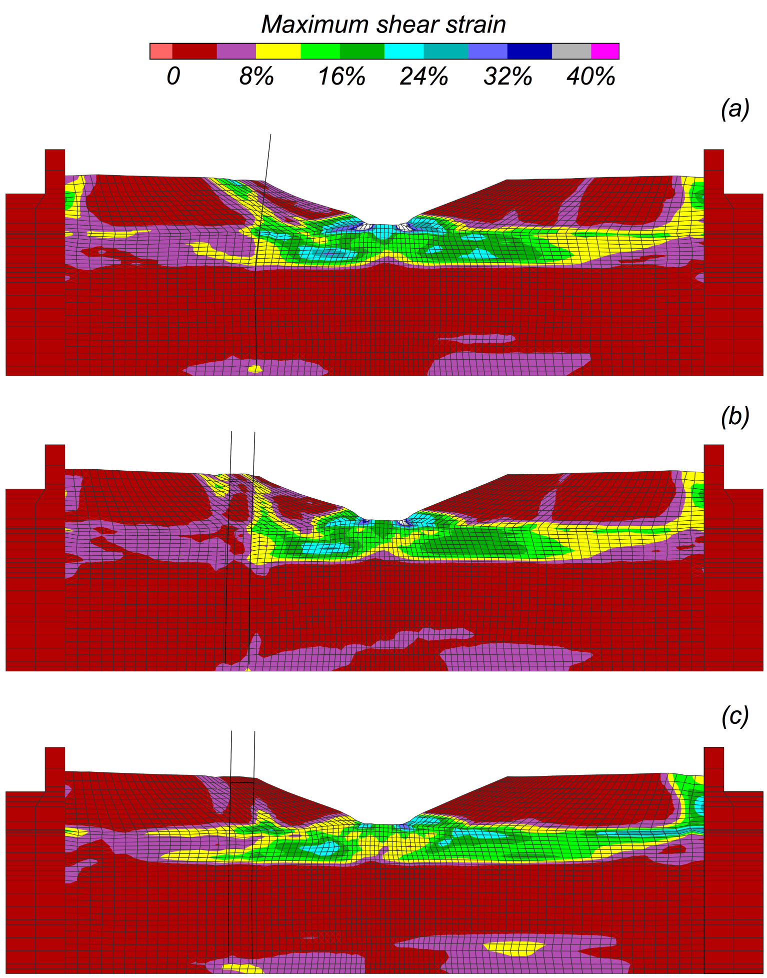

Figure 5. Deformed meshes after shaking: (a) Kobe_1x6 (b) Kobe_2x4, and (c) Sine_2X4

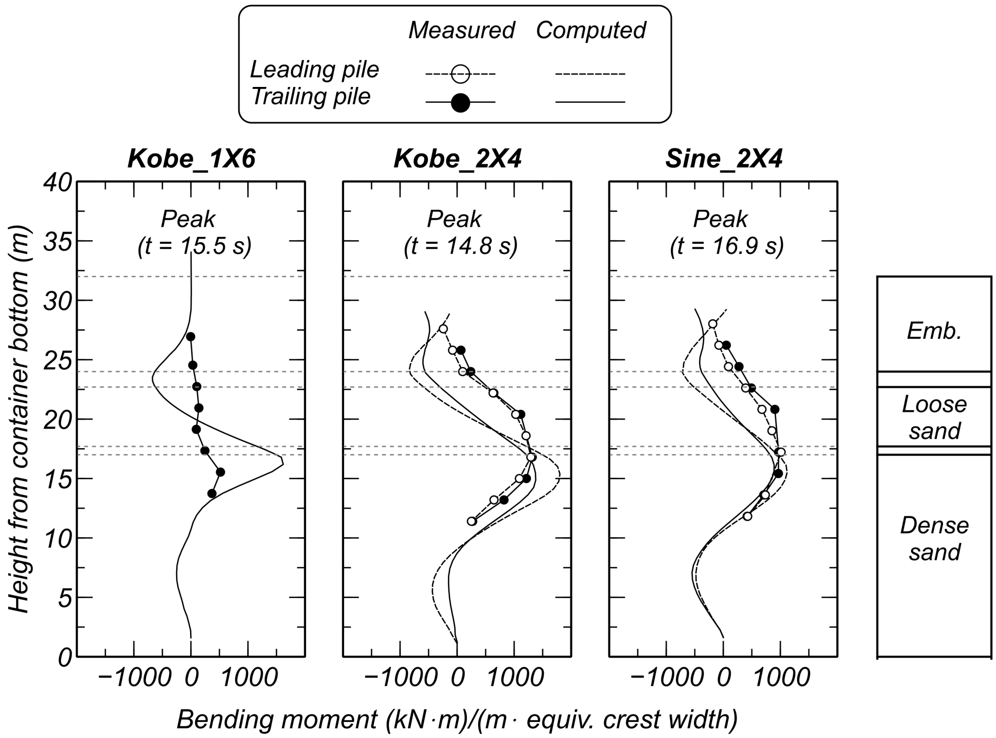

Figure 6. Measured and computed pile bending moments at the time of peak moment

Acknowledgments

The centrifuge tests were performed with funding from the Pacific Earthquake Engineering Research (PEER) Center; through the Earthquake Engineering Research Centers Program of the National Science Foundation, under Contract No. 2312001; and through the PEER Lifelines program, under Contract No. 65A0058. The contents of this paper do not necessarily represent a policy of either agency or an endorsement by the state or federal government.

References

Armstrong RJ, Boulanger RW, Beaty MH. "Liquefaction effects on piled bridge abutments: Centrifuge tests and numerical analyses." *J. Geotech. and Geoenv. Engrg*., ASCE, 2013; **139**(3), 433-443.

Armstrong RJ, Boulanger RW, Beaty MH. "Equivalent static analyses of piled bridge abutments affected by *earthquake-induced liquefaction." J. Geotech. And Geoenv. Engrg., ASCE, 2014;* ***140****(8).*

Beaty MH, Byrne PM. *UBCSAND constitutive model: Version 904aR.* Documentation Report: UBCSAND Constitutive Model on Itasca UDM Web Site, 2011; accessed February 2011.

Boulanger RW, Ziotopoulou K. "Formulation of a sand plasticity plane-strain model for earthquake engineering applications." Journal of Soil Dynamics and Earthquake Engineering, 2013; ***53****: 254-267.*

Boulanger RW, Ziotopoulou K. *"PM4Sand (Version 3): A sand plasticity model for earthquake engineering applications."* UCD/CGM-15/01, Ctr. for Geotech. Modeling, University of California, Davis, CA, 2015.

Byrne P, Park S, Beaty M, Sharp M, Gonzalez L, Abdoun T. "Numerical modeling of liquefaction and comparison with centrifuge tests." *Canadian Geotechnical Journal*, 2014; **41**(2).

Chang D, Gulerce U, Armstrong R, Khosravifar A, Boulanger R, Kutter B. *"Pile pinning effects on a bridge abutment in laterally spreading ground during earthquakes: centrifuge data report for DDC03."* UCD-CGMDR-06-01, Center for Geotechnical Modeling, University of California, Davis, CA, 2017.

Cubrinovski M, Winkley A, Haskell J, Palermo A, Wotherspoon L, Robinson K, Bradley B, Brabhaharan P, Hughes M. "Spreading-induced damage to short-span bridges in Christchurch, New Zealand." *Earthquake Spectra*, 2014; **30**(1): 57-83.

Gulerce U, Armstrong R, Khosravifar A, Boulanger R, Kutter B. *"Pile pinning effects on a bridge abutment in laterally spreading ground during earthquakes: centrifuge data report for UGU01*." UCD-CGMDR-06-02, Center for Geotechnical Modeling, University of California, Davis, CA, 2007a.

Gulerce U, Armstrong R, Brandenberg S, Khosravifar A, Boulanger R, Kutter B. *"Pile pinning effects on a bridge abutment in laterally spreading ground during earthquakes: centrifuge data report for UGU02."* UCD-CGMDR-06-03, Center for Geotechnical Modeling, University of California, Davis, CA, 2007b.

Itasca. *"FLAC, Fast Lagrangian Analysis of Continua, User's Guide, Version 7.0."* Itasca Consulting Group, Inc., Minneapolis, MN, 2011.

*K*amai R, Boulanger RW. "Simulations of a centrifuge test with lateral spreading and void redistribution effects." *Journal of Geotechnical and Geoenvironmental Engineering*, ASCE, 2013; **139**(8): 1250-1261.

Ziotopoulou K, Boulanger RW. *"Calibration and implementation of a sand plasticity plane-strain model for earthquake engineering applications."* J. Soil Dynamics and Earthquake Engineering, 2013; **53**: 268-280,